

Unconventional superconductivity originating from disconnected Fermi surfaces in the iron-based compound

Hideo Aoki^a

^aDepartment of Physics, University of Tokyo, Tokyo 113-0033, Japan

Abstract

The iron-based $\text{LaFeAsO}_{1-x}\text{F}_x$ recently discovered by Hosono's group is a fresh theoretical challenge as a new class of high-temperature superconductors. Here we describe the electronic structure of the material and the mechanism of superconductivity. We start with constructing a tight-binding model in terms of the maximally localized Wannier orbitals from a first-principles electronic structure calculation, which has turned out to involve all the five Fe 3d bands. This is used to calculate the spin and charge susceptibilities with the random phase approximation. The spin susceptibility has peaks around $k = (\pi, 0); (0, \pi)$ arising from a nesting across disconnected Fermi surface pockets. We have then plugged the susceptibilities into the linearised Eliashberg equation. For the doping concentration $x = 0.1$, we obtain an unconventional s-wave pairing, which is roughly an extended s in that the gap changes sign between the Fermi pockets, but the gap function is actually a 5 × 5 matrix. Its experimental implications are also discussed.

Key words: iron-based superconductor, electron mechanism of superconductivity, extended s pairing

1. Introduction

The discovery of the high- T_c cuprate was epoch-making in that the material has opened a new avenue of the correlated electron systems and associated electron mechanism of superconductivity. However, we are still some way from a complete understanding, and a new class of materials has been desired, which would be a testbench for various ideas and concepts, both experimental and theoretical, in the electron correlation. So the discovery of superconductivity in the iron-based pnictide LaFeAsO doped with fluorine ($\text{LaFeAsO}_{1-x}\text{F}_x$) discovered by Hosono's group [1] is particularly welcome. Indeed, this is the first non-copper family of compounds whose T_c exceeds 50 K in the subsequent studies (Fig. 1).

This immediately stimulates renewed interests in the electron mechanism of high T_c superconductivity. Especially interesting, in our view, is that the way in which the correlation effects such as magnetism and superconductivity appear in strongly correlated electron systems is very sensitive to the underlying band structure. We can envisage to exploit the "fermionology in correlated electron systems" to explore the possibility of manipulating superconductivity by choosing the shape of the Fermi surface.[2]

In this paper we first briefly look at unconventional su-

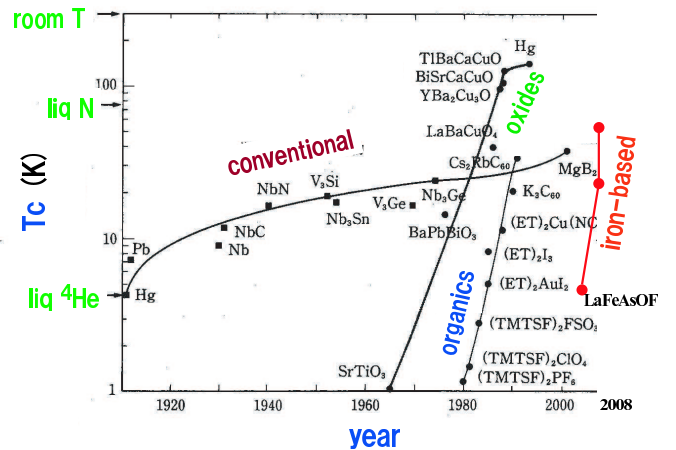


Fig. 1. (color online) T_c against calendar year for various classes of superconductors.

perconductivity as a background. We then give a description of the electronic structure and a possible mechanism for superconductivity for the iron-based compound. Theoretically, the material turns out to have a curious multiband structure, with the Fermi surface comprising some pockets. In order to investigate the pairing mechanism, here we first construct an electronic model for the iron-based com-

pound with the "downfolding" based on a first-principles electronic structure calculation. The minimum model turns out to contain all the d orbitals. We then apply the d -band random phase approximation (RPA) to solve the Eliashberg equation. We conclude that a nesting between multiple Fermi surface (pockets) results in a development of peculiar spin fluctuation modes, which in turn realises an unconventional (roughly extended s) pairing.[3] The result is intriguing as one realisation of the idea of fermiology in general and the idea of the "disconnected Fermi surface" in particular[4]. Finally we shall summarise that, as opposed to the strongly correlated, half-filled, one-band cuprate as a doped Mott insulator, the iron compound is moderately correlated, dilute multi-band system. An outlook for the iron compound is also given.

2. Unconventional superconductivity

After the discovery of the cuprate, a number of other classes of superconductors have been discovered, among which are the ruthenate, the cobaltate, the Hf compound and the Ce compound. These have given a strong impetus towards the study of electron mechanism of superconductivity. In the conventional mechanism, superconductivity arises from the electron-electron attraction mediated by phonons, where $T_C \sim 10$ K is one order of magnitude smaller than the phonon energy $\hbar\omega_D \sim 100$ K. In the electron mechanism, superconductivity arises from the electron-electron repulsion, where spin and charge fluctuations mediate pairing with $T_C \sim 100$ K, two orders of magnitude smaller than the electronic energy $E_F \sim 10000$ K.

The pairing from repulsive interactions itself is nothing strange, if we allow anisotropic pairing symmetries accompanied by anisotropic gap functions, $\Delta(\mathbf{k})$. The point is, if we look at the BCS gap equation,

$$\Delta(\mathbf{k}) = \sum_{\mathbf{k}'} V(\mathbf{k}; \mathbf{k}') \frac{\Delta(\mathbf{k}')}{2E(\mathbf{k}')} \tanh \frac{E(\mathbf{k}')}{2k_B T} ; \quad (1)$$

where $V(\mathbf{k}; \mathbf{k}')$ is the pairing interaction, we can immediately recognise that a repulsion acts as an attraction when $\Delta(\mathbf{k})$ changes sign across the typical momentum transfer (usually dictated by the dominant spin fluctuation mode). This is what is happening in the cuprate with a d -wave pairing.

The question, then, is "why is $T_C \sim \frac{1}{100} E_F$ in the electron mechanism is so low?", as most transparently displayed by Uemura's experimental plot for T_C against T_F [5]. Theoretically, there are good reasons why T_C is low: (a) the effective attraction mediated by the fluctuation is much smaller than the bare (repulsive) interaction. (b) Quasi-particles are short-lived due to large self-energy corrections from the electron correlation, and (c) the prerequisite anisotropy in pairing with the gap-function nodes, which usually intersect the Fermi surface, suppresses T_C . We can then think of how we can manipulate these factors. Several years ago Kuroki and Arita [4] have proposed that we

can overcome the difficulty (c) by considering disconnected Fermi surfaces, on which we can pierce the nodes in between the Fermi pockets. Each pocket is then fully gapped, with opposite signs across the pockets. While the disconnected Fermi surfaces may first seem artificial, it has been recognised that they actually occur in real materials including TM TSS [6] and Co compounds [7].

As for the spatial dimensionality, Arita et al have shown that two-dimensional (layered) systems are more favourable than 3D ones for the spin-fluctuation mediated superconductivity for ordinary lattices [8]. This is because the fraction of the phase space over which the pairing interaction is appreciable is larger in 2D. The result, also obtained by Monthoux and Lonzarich [9], agrees with the empirical fact that recently discovered superconductors (cuprates, Co compound, Hf compound, CeCoIn₅, etc) are mostly layer-structured. The iron-based compound has turned out to be no exception.

3. LaFeAsO

LaFeAsO has a tetragonal layered structure (Fig.2), where each Fe layer comprises edge-shared FeAs₄ tetrahedra with Fe atoms forming a square lattice. Since the bands around E_F have negligible LaO-layer components, we can concentrate on the Fe layer. The experimentally determined lattice constants are $a = 4.03552$ Å and $c = 8.7393$ Å, with two internal coordinates $z_{La} = 0.1415$ and $z_{As} = 0.6512$. In the experimentally obtained phase diagram in the original discovery [1] and in an SR study [10] (arXiv:0806.3533) the (collinear; see below) SDW is taken over by the superconducting phase as the F -doping level is increased.

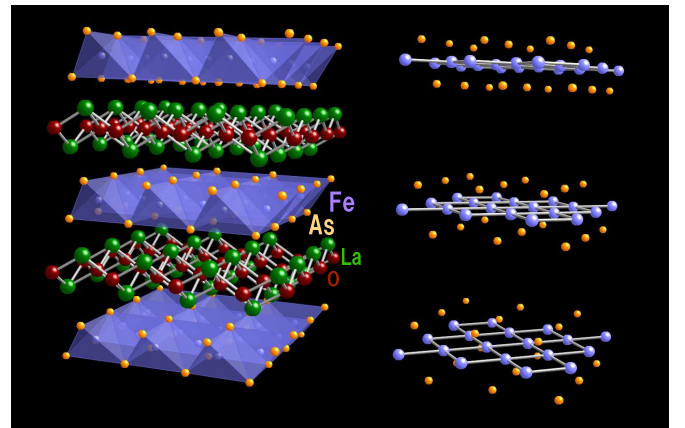


Fig. 2. (color online) Crystal structure of the LaFeAsO. The right panel picks up the FeAs layers.

After the discovery of superconductivity, a surge of intensive studies on the material has ensued. Since it is impossible to survey them here, let us here mention only a few examples with an extremely partial list of references. In the iron-based family, various compounds have been shown to exhibit superconductivity, among which are NdFeAsO_{1-x}F_x [11], PrFeAsO_{1-x}F_x [12],

GdFeAsO_{1-y} [13], SmFeAsO_{1-x}F_x [14], with T_C now exceeding 56 K. Pressure effects have been studied for LaFeAsO_{1-x}F_x [15], NdFeAsO_{1-y} [16], etc. Superconductivity has also been found in iron-based materials with different layered structures that include BaFe₂As₂ [17] and FeSe [18].

We can first itemise the experimental results that indicate unconventional SC :

- (i) NMR, where absence of coherence peak, $1/T_1 \propto T^3$, etc have been observed. [19]
- (ii) Electronic specific heat C_{el}/T , etc has been observed. [20]
- (iii) Point-contact tunnelling, where zero-bias peak, indicative of a sign change across Fermi pockets, etc have been observed. [21]
- (iv) SR is used to measure the superfluid density. [22] Especially interesting is the Uemura plot, in which the iron compound is shown to reside more or less on the Uemura line, so in this sense the iron compound is at least as good as the cuprate.
- (v) Raman spectra indicate a weak electron-phonon coupling. [23]
- (vi) $H_{c2}; H_{c1}$ indicate a two-gap behaviour. [24]
- (vii) Photoemission spectroscopy, [25] and more recently ARPES depict the Fermi surface, gap, etc [26].

Experimental results for magnetic properties, especially interesting in relation to the mechanism of superconductivity, include the following :

- (i) Mossbauer studies indicate a magnetic transition temperature T_N = 140 K with a magnetic moment M = 0.25 – 0.35 μ_B (at T = 4 K) [27,28].
- (ii) Neutron diffraction studies indicate a collinear (stripe) SDW (see Fig.5) in Fe moments with T_N = 134 K, M = 0.35 μ_B (at T = 8 K) [29].
- (iii) SR suggests a spontaneous muon spin precession below T_N = 138 K [30].
- (iv) NMR shows T_N = 142 K [31].
- (v) Transport measurements indicate an anomaly around T = 140 – 150 K [32].
- (vi) X-ray diffraction shows a structural phase transition (tetragonal \rightarrow orthorhombic) at \sim 150 K [33], which is close to, but somewhat deviates from, the magnetic transition temperature.

Theoretically, if we first look at the periodic table, copper, in its Cu²⁺ state, has a 3d⁹ electron configuration. This makes the cuprate one-band, nearly half-filled system, where we have a spin 1/2 at each site with strong antiferromagnetic fluctuations. By contrast, Fe, located in the middle of the table, has a 3d⁶ configuration, so multiple d bands tend to be involved. A point of interest is that we usually associate iron with ferromagnetism rather than with superconductivity [34], and how the multiband structure for the iron compound gives rise to superconductivity.

We then definitely require the electronic band structure to begin with.

- { Several groups have obtained the band structure [35,36,37].
- { Theoretical suggestions on magnetic properties include

an LDA + DMFT study which indicates no local moment for the Hund's coupling J_H < 0.35 eV [38].

- { An ab initio (cRPA) calculation estimates J_H \sim 0.2 eV. [39]
- { An itinerant character of the compound suggested from several papers [41].
- { Sensitivity of the electronic structure against the Fe-As distance has been suggested in a maximally localised Wannier study that incorporates As 4p orbitals [42].

4. Model construction

First two papers that study the mechanism of superconductivity are by Mazin et al [40] and by Kuroki et al [3]. The former starts from the Fermi surface and constructs an effective RPA treatment for the spin susceptibility $\chi_0(q) = [J(q) + \chi_0(q)]$ to predict the collinear SDW and an extended s-wave pairing. The latter starts with a model building via downfolding to actually solve Eliashberg's equation for the full ve-band model. Here we briefly describe this approach.

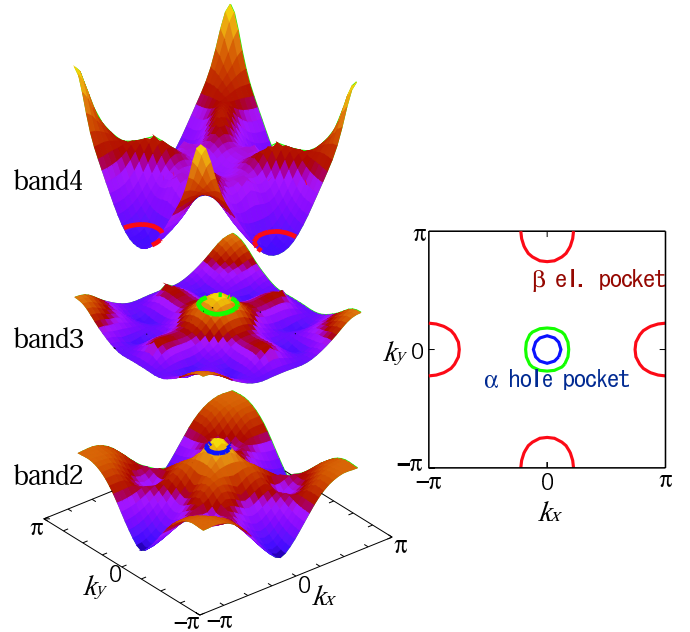


Fig. 3. (color online) Left panel: The dispersion of the three bands that intersect E_F in LaFeAsO_{1-x}F_x with 10 % doping (x = 0.1). Right panel: Fermi surface (with the inter-layer hopping ignored).

The approach starts from a band structure (Figs.3, 4) with the density-functional approximation with plane-wave basis [43] for constructing the model. For that, we have employed a standard procedure with maximally localized Wannier functions (MLWFs) [44]. These MLWFs, centred at the two Fe sites in the unit cell, have ve orbital symmetries (orbital 1: d_{3z²-r²}, 2: d_{xz}, 3: d_{yz}, 4: d_{x²-y²}, 5: d_{xy}). Due to the tetrahedral coordination of As, there are two Fe atoms per unit cell, and X;Y;Z refer to those in the original unit cell. The two Wannier orbitals in each unit cell are equivalent in that each Fe atom has the same local arrangement of other atoms. We can thus take a unit cell

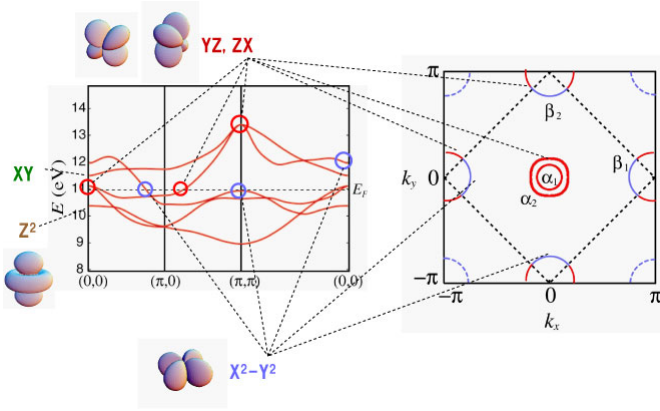


Fig. 4. (color online) The band structure of the ve-band model in the unfolded BZ, where the inter-layer hoppings are included. Orbital character is indicated for the bands and for the Fermi surface (right panel), with the original (dashed lines) and the unfolded (solid) BZ indicated). Bottom panels depict (two equivalent realisations of) the colinear SDW.

that contains only one orbital per symmetry by unfolding the Brillouin zone (BZ), and we end up with an effective ve-band model on a square lattice, where x and y axes are rotated by 45 degrees from X - Y , to which we refer for all the wave vectors hereafter. We define the band filling n as the number of electrons/number of sites (e.g., $n = 10$ for full filling). The doping level x in $\text{LaFeAsO}_{1-x}\text{F}_x$ is related to the band filling as $n = 6 + x$.

The ve bands are heavily entangled as shown in Fig. 4, which reflects hybridisation of the ve 3d orbitals due to the tetrahedral coordination of As 4p orbitals around Fe. Hence we conclude that the minimal electronic model requires all the ve bands. [45] In Fig. 4, the Fermi surface for $n = 6.1$ (corresponding to $x = 0.1$) obtained by ignoring the inter-layer hoppings is shown in the two-dimensional unfolded BZ. The shape of the Fermi surface is now being experimentally detected with ARPES. [26]

The Fermi surface consists of four pieces (pockets in 2D when the inter-layer hoppings are neglected): two concentric hole pockets (denoted as β_1, β_2) centred around $(k_x; k_y) = (0; 0)$, two electron pockets around $(\pi; 0)$ (β_1) or $(0; \pi)$ (β_2), respectively. β_1 (β_2) corresponds to the Fermi surface around the Z (M) A line (in the original BZ) in Singh's band calculation. [36] In addition, we notice that a portion of the band near $(\pi; \pi)$ is flat and touches the E_F at $n = 6.1$, so that the portion acts as a "quasi-Fermi surface" around $(\pi; \pi)$. The orbital character is again entangled: β_1 and portions of β_2 near BZ edge has mainly d_{xz} and d_{yz} character, while the portions of β_2 away from the BZ edge and β_1 have mainly $d_{x^2-y^2}$ orbital character.

5. Five-band RPA results for magnetism and pairing

Having constructed the model, we move on to the RPA calculation in the 2D model. For the many-body part of the Hamiltonian, we consider the standard interaction

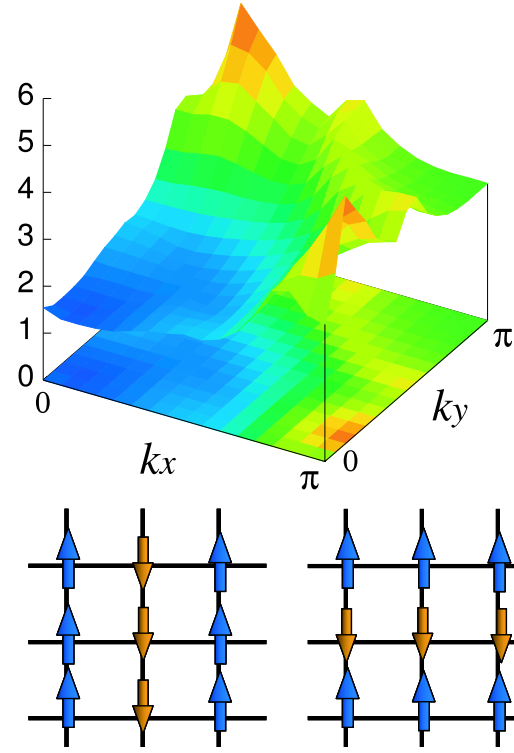


Fig. 5. (color online) 5-band RPA result for the spin susceptibility for 10% doped $\text{LaFeAsO}_{1-x}\text{F}_x$ for $U = 1.2, U^0 = 0.9, J = J^0 = 0.15$, and $T = 0.02$ (in eV). Bottom panels depict the colinear SDW for $\mathbf{k} = (0; 0); (0; \pi)$.

terms that comprise the intra-orbital Coulomb U , the inter-orbital Coulomb U^0 , the Hund's coupling J , and the pair-hopping J^0 . The modification of the band structure due to the self-energy correction is not taken into account. For the ve-band model, Green's function is a 5×5 matrix in the orbital representation, while each of the spin and orbital susceptibilities $\chi_{ll'; 12; 13; 14}$ ($l = 1; \dots; 5$) is a 25×25 matrix. The Green's function and the effective pairing interactions, obtained from the susceptibilities, are plugged into the linearised Eliashberg equation, and the gap function as a 5×5 matrix is obtained along with the eigenvalue. 32×32 k -point meshes and 1024 Matsubara frequencies are taken. We find that the spin fluctuations dominate over orbital fluctuations as far as $U > U^0$, so we can characterise the system with the spin susceptibility. We denote the largest eigenvalue of the spin susceptibility matrix for $l = 0$ as $\chi_s(\mathbf{k})$. The gap function matrix at the lowest Matsubara frequency is transformed into the band representation by a unitary transformation, and its diagonal element for band i is denoted as $\Delta_i(\mathbf{k})$.

Let us look at the result for the spin susceptibility χ_s for $U = 1.2, U^0 = 0.9, J = J^0 = 0.15$, and $T = 0.02$ (all in units of eV) in Fig. 5. The spin susceptibility has peaks around $(k_x; k_y) = (0; 0), (0; \pi)$ (i.e., a colinear SDW), which reflects the Fermi surface nesting around $(\pi; 0); (0; \pi)$ across β_1 and β_2 and also β_2 in Fig. 4. The spin structure is consistent with the neutron scattering experiments in which the colinear structure is observed at low temperatures for

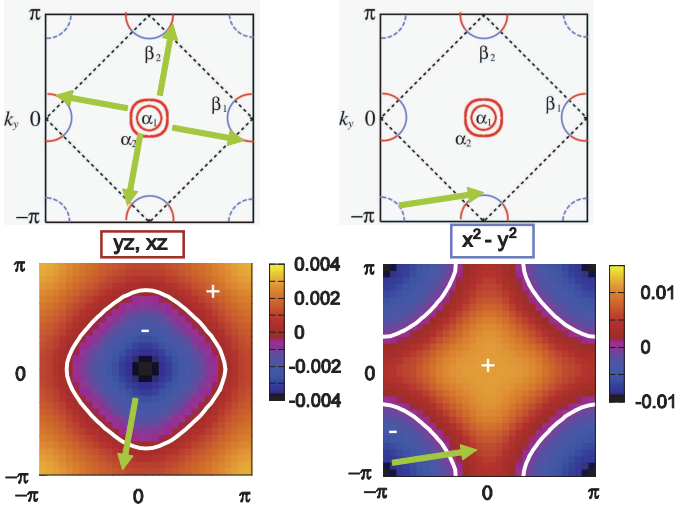


Fig. 6. (color online) Bottom panels: Diagonal elements of the gap function matrix in the orbital representation for the $XZ; YZ$ (left) and $X^2 - Y^2$ (right) in the 5-band RPA for 10% doped $\text{LaFeAsO}_{1-x}\text{Fx}$ for the same parameter set as in the previous figure. Nesting vectors are indicated in the top panels.

the undoped case.[29]

For superconductivity, we show in Fig.6 the diagonal elements of the gap function matrix for orbitals d_{yz} , d_{zx} , and $d_{x^2 - y^2}$. The gap is a curious extended s-wave, [40,3] where the gap changes sign across the nesting vector $(\pi; 0); (0; \pi)$ at which the spin fluctuations develop. The sign change is analogous to those in models studied by Bulut et al., [46] and Kuroki and Arita [4]. To be more precise for the multiband system, the magnitude of gap of the $d_{x^2 - y^2}$ orbital turns out to be large compared to other orbitals, which indicates that the $d_{x^2 - y^2}$ orbitals play the main role in the superconductivity. The extended s ($\cos k_x + \cos k_y$ in k space) should look in real space as depicted in Fig.7.

However, we have to be careful in analysing the gap, since we have a multiband system at hand, where the band character changes along the Fermi surface (Fig.4). When we concentrate on the main component ($d_{x^2 - y^2}$ orbitals) of the gap function, the magnitude of the gap varies along the Fermi surface, which is because the character of the Fermi surface changes, as we approach the BZ boundary, to d_{yz} , d_{zx} for which the gap is smaller. More importantly, we should always be aware that the gap function is a 5x5 matrix, where off-diagonal elements are rather significant due to the heavy entanglement of the bands. This should have experimental implications for various quantities. An importance of matrix character of the gap is illustrated in Fig.8 that displays the quantity $(\hat{\gamma})_{44}$, where $\hat{\gamma}$ is the gap matrix and 44 denotes the diagonal element of band 4. As shown in the figure, this quantity is fully gapped over the entire BZ. A remnant of the nodal lines of the diagonal element appears as a dip that intersects the Fermi surface, which may look like a node e.g. at not low enough temperatures. The degree of the variation of the gap may be determined experimentally from e.g. tunnelling spectroscopy

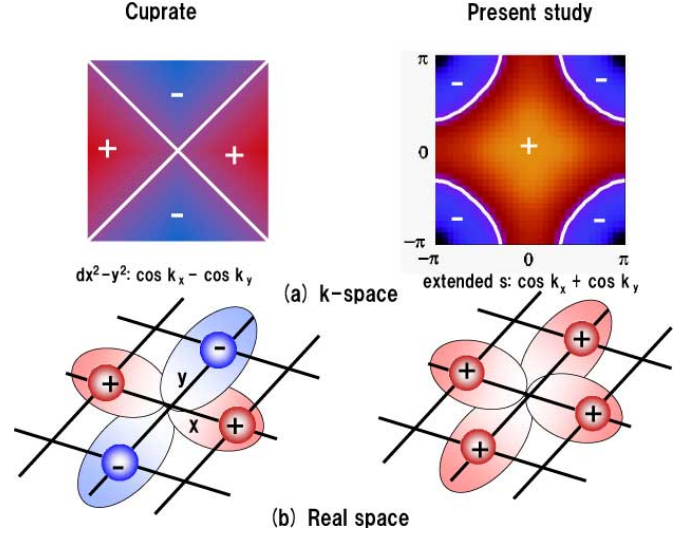


Fig. 7. (color online) Gap function symmetry is schematically shown for the cuprate (left panels) and the present result for the iron compound (right), in the k-space (top panels) and in the real space (bottom).

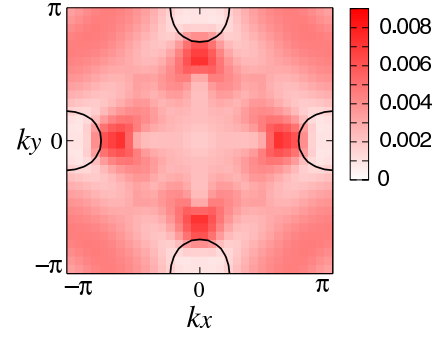


Fig. 8. (color online) 5-band RPA result for the gap function, $(\hat{\gamma}^y)_{44}$ for the same parameter set as in the previous figures.

or ARPES. Also interesting is how the penetration depth, $\lambda = \sqrt{m/n_s}$ with n_s being the superfluid density in the one-band system, should be given in the multiband system.

6. Conclusion

To summarise, we have very briefly reviewed the iron compound, and then described a theory in which a five-band electronic model is constructed as a minimum microscopic model. Applying a five-band RPA to this model, we have found that spin fluctuation modes around $(\pi; 0); (0; \pi)$ develop due to the nesting between disconnected Fermi surfaces. Based on the linearised Eliashberg equation, we have concluded that spin fluctuation modes realise an unconventional, extended s-wave pairing, where the diagonal elements of the gap matrix change sign across the nesting vector. The $d_{x^2 - y^2}$ orbital is the main component in the superconductivity gap function, although the gap function as a 5x5 matrix may be important.

Overall, while the cuprate is strongly correlated ($U > W$ with W the band width), one-band and nearly half-

lled system, the iron compound is moderately correlated (U W) [39], multi-band and dilutely lled system. This poses a challenging problem of whether the iron compound can exceed the cuprate. Relevance to experimental results, especially SR including the Uemura plot, is also a pressing future problem.

The work described here is a collaboration with Kazuhiko Kuroki, Seiichiro Onari, Ryotaro Arita, Hidetomo U sui, Yukio Tanaka and Hiroshi Kontani. Numerical calculations were performed at the facilities of the Information Technology Center, University of Tokyo, and also at the Supercomputer Center, ISSP, University of Tokyo. This study has been supported by Grants-in-Aid for Scientific Research from MEXT of Japan and from the Japan Society for the Promotion of Science.

References

- [1] Y. Kamihara et al.: J. Am. Chem. Soc. 130 (2008) 3296; H. Takahashi et al, Nature 453, 376 (2008).
- [2] H. Aoki in T. B. Randes et al (ed.): Lecture Notes in Physics 630 (Springer, 2003), p.219; H. Aoki, Physica C 437-438, 11 (2006); H. Aoki in Condensed Matter Theories 21 ed. by H. Akaï et al, (Nova Science, 2007).
- [3] K. Kuroki, S. Onari, R. Arita, H. U sui, Y. Tanaka, H. Kontani and H. Aoki, Phys. Rev. Lett. 101, 087004 (2008).
- [4] K. Kuroki and R. Arita: Phys. Rev. B 64 (2001) 024501; Phys. Rev. B 66 (2002) 184508.
- [5] Y. Uemura et al, Nature 352, 605 (1991); Phys. Rev. Lett. 66, 2665 (1991); J. Phys.: Condens. Matter 16, S4515 (2004).
- [6] K. Kuroki, R. Arita and H. Aoki, Phys. Rev. B 63, 94509 (2001).
- [7] K. Kuroki et al.: Phys. Rev. B 73 (2006) 184503.
- [8] R. Arita et al, Phys. Rev. B 60, 14585 (1999).
- [9] P. Monthoux and G. G. Lonzarich, Phys. Rev. B 59, 14598 (1999).
- [10] H. Luetkens et al, arXiv:0804.3115, 0806.3533.
- [11] Z. A. Ren et al, arXiv:0803.4234.
- [12] Z. A. Ren et al, arXiv:0803.4283.
- [13] J. Yang et al, Supercond. Sci. Tech. 21, 82001 (2008); P. Cheng et al, arXiv:0804.0835; C. Wang et al, arXiv:0804.4290.
- [14] Z. A. Ren et al, arXiv:0804.2053.
- [15] H. Takahashi et al, Nature 453, 376 (2008).
- [16] N. Takeshita et al: J. Phys. Soc. Jpn 77, 075003 (2008).
- [17] M. Rotter et al, arXiv:0805.4630.
- [18] F. C. Hsu et al, arXiv:0807.2369.
- [19] Y. Nakai et al, arXiv:0804.4765; K. Ahilan, et al, Phys. Rev. B, in press.
- [20] G. Mu et al, Chin. Phys. Lett. 25, 2221 (2008).
- [21] L. Shan et al, Europhys. Lett. 83 (2008) 57004.
- [22] Ref.[10]; A. J. Drew et al, arXiv:0805.1042; R. Khasanov et al, arXiv:0805.1923; J. P. Carlo et al, arXiv:0805.2186; A. A. Czele et al, arXiv:0807.1044; T. Goko et al, arXiv:0808.1425.
- [23] H. Luetkens et al, arXiv:0804.3115; K. Ahilan et al, arXiv:0804.4026; V. G. Hadjiev et al, arXiv:0804.2285.
- [24] F. Hunte et al, Nature 453, 903 (2008); C. Ren et al, arXiv:0808.0805.
- [25] T. Sato et al, J. Phys. Soc. Jpn 77, 063708 (2008); W. M. Alae et al, J. Phys. Soc. Jpn, in press.
- [26] L. Zhao et al, arXiv:0807.0398; C. Liu et al, arXiv:0806.2147, 3453, 4806; D. H. Lu et al, arXiv:0807.2009; H. Ding et al, Europhys. Lett. 83, 47001 (2008).
- [27] S. Kaito et al, arXiv:0805.0041.
- [28] H. H. Klauss et al, arXiv:0805.0264.
- [29] C. de la Cruz et al, Nature 453, 899 (2008).
- [30] Ref.[28]; H. Luetkens et al, arXiv:0804.3115.
- [31] Y. Nakai et al, arXiv:0804.4765.
- [32] Refs.[1,28]; Dong et al, arXiv:0803.3426.
- [33] T. Nomura et al, arXiv:0804.3569.
- [34] Elemental Fe is known to become a superconductor with $T_c \sim 2$ K in high pressures [K. Shimizu et al, Nature 412, 316 (2001)], but even then SC appears after ferromagnetism vanishes.
- [35] S. Lebegue, Phys. Rev. B 75, 035110 (2007).
- [36] D. J. Singh and M. -H. Du: Phys. Rev. Lett. 100 (2008) 237003.
- [37] S. Ishibashi et al, J. Phys. Soc. Jpn 77, 53709 (2008).
- [38] K. Haule et al, arXiv:0805.0722.
- [39] K. Nakamura et al, arXiv:0806.4750.
- [40] I. I. Mazin et al, arXiv:0803.2740.
- [41] Refs.[3,40]; I. I. Mazin et al, arXiv:0806.1869; Z. P. Yin et al, arXiv:0804.3355.
- [42] V. Vildosola et al, arXiv:0806.3285.
- [43] S. Baroni et al, <http://www.pwscf.org/>. Here we adopt the exchange correlation functional introduced by J. P. Perdew et al [Phys. Rev. B 54 (1996) 16533], and the wave functions are expanded by plane waves up to a cutoff energy of 40 Ry. 10^3 k-point meshes are used with the special points technique by H. J. Monkhorst and J. D. Pack [Phys. Rev. B 13 (1976) 5188].
- [44] N. Marzari and D. Vanderbilt, Phys. Rev. B 56 (1997) 12847; I. Souza et al, Phys. Rev. B 65 (2002) 035109. The Wannier functions are generated by the code developed by A. A. Mosto et al (<http://www.wannier.org/>) for the energy window -2 eV $< \epsilon_k - E_F < 2.6$ eV, where ϵ_k is the eigenenergy of the Bloch states and E_F the Fermi energy.
- [45] Subsequently several theoretical papers have tried to reduce the number of orbitals into two ($d_{yz} + d_{xz}$) [M. M. Korshunov et al, arXiv:0804.1793; X. L. Qi et al, arXiv:0804.4332; S. Raghu et al, Phys. Rev. B 77, 220503 (2008); M. Daghofer et al, arXiv:0805.0148] or three ($d_{yz} + d_{xz} + d_{x^2-y^2}$) [P. A. Lee and X. G. Wen, arXiv:0804.1739], but they do not reproduce the full Fermi surface.
- [46] N. Bulut et al: Phys. Rev. B 45 (1992) 5577.